

Exploring the dark side of the top Yukawa

Sonia El Hedri,¹ Patrick J. Fox,² and Jay G. Wacker¹

¹ *SLAC, Stanford University, Menlo Park, CA 94025 USA*

² *Theoretical Physics Department, Fermi National Accelerator Laboratory, Batavia, IL 60510, USA*

Abstract

We investigate simple extensions of the Standard Model that could lead to the negative values of the top Yukawa coupling still allowed by the ATLAS Higgs results. Integrating out tree-level new physics generates dimension six operators that can lead to large changes to the top Yukawa couplings. If the top Yukawa coupling is negative, there is new physics beneath the TeV scale. We illustrate the simplest models still allowed by current searches.

1. INTRODUCTION

Since the discovery of a 125 GeV Higgs boson by ATLAS and CMS in July 2012 [1, 2], measurements of the Higgs coupling to Standard Model particles have become a new way to probe new physics [3–22]. Although the current measured values of these couplings are consistent with the Standard Model (SM) predictions [23, 24], ATLAS’s central value for $gg \rightarrow h \rightarrow \gamma\gamma$ [25] is significantly above the SM value, so much that there are two distinct allowed regions for the inferred top Yukawa coupling [23]. The second region is distinctive because in this region the Yukawa coupling of the Higgs to the top quark has negative values. This paper will discuss the physics necessary to accommodate this second region. Since this region is in tension with the CMS $gg \rightarrow h \rightarrow \gamma\gamma$ results, this paper will only use the ATLAS and Tevatron [26] results.

One possible interpretation of this new region of parameter space is the existence of a new colored and/or charged particle which runs in loops for $h \rightarrow gg$ and $h \rightarrow \gamma\gamma$. Such a scenario has been considered in [27, 28] and has been severely constrained in [29]. A different approach is adopted here, where minimal models which generate a negative Yukawa coupling at tree-level are studied.

These minimal models, however, need to accommodate large changes to the top Yukawa coupling and will therefore be extremely constrained by collider searches. Integrating out tree-level physics, the lowest dimensional effective operator which could contribute to the value of the top Yukawa coupling is of the form

$$\mathcal{L}_{\text{eff}}^{(1)} = \frac{Y^3}{\Lambda^2} \left(H^\dagger H - \frac{v^2}{2} \right) (H \bar{q}_3 u_3^c + h.c.) . \quad (1)$$

This operator does not change the top mass and leads to tree-level contributions to the top Yukawa coupling such that

$$y_t^{\text{eff}} = \frac{\sqrt{2}m_t}{v} + \frac{Y^3}{\sqrt{2}} \frac{v^2}{\Lambda^2} . \quad (2)$$

This shows that, in order for y_t^{eff} to take large negative values, Λ needs to remain close to the electroweak scale and Y must be of order one. Thus, generating the effective operator shown in Eq. 1 then requires introducing new sub-TeV particles.

This dimension six operator arises in three simple scenarios, where the new particles can be

1. new vector-like fermions: two Dirac top partners, Q and U (Fig. 1-a)
2. both fermions and scalars: one fermionic top quark partner U and one scalar singlet S (Fig. 1-b)
3. new electroweakly charged scalars (Fig. 1-c).

which lead to the diagrams shown in Fig. 1. In order to maximize the effective operator contribution to the top Yukawa, these particles would have to be light and have large couplings to the Higgs boson and the top. Therefore, negative top Yukawas require significant changes to sub-TeV physics that have been searched for by Tevatron and LHC searches. Due to the large values of the couplings of the new particles to the SM, models with negative top Yukawas also lead in most cases to low scale Landau poles.

We discuss below the regions still allowed by the Higgs searches at ATLAS, before going on to describe possible models to realize the negative top Yukawa solutions, the so called “dark side”. In Section 2 we discuss models that introduce new vector-like top quark partners. In Section 3 we describe models with extra Higgs fields. Specifically, we consider a two Higgs doublet model [30–32] where both Higgses couple to the top quark, an arbitrary number of Higgs doublets, and finally a model involving higher $SU(2)$ representations. We show that in all but the last case these models cannot generate a sufficiently negative top Yukawa to reach the dark side. The last model discussed can and has many new light states that can be searched for at the LHC.

1.1. ATLAS searches

Throughout this paper, there are two important Higgs couplings that will be modified with respect to their SM values: the Higgs couplings to the top quark and to vector bosons. Their deviations with respect to their SM values, κ_t and κ_V , are defined by

$$\mathcal{L} \supset \frac{m_t}{\sqrt{2}v} \kappa_t h t \bar{t} + \kappa_V \frac{g}{\sqrt{2}v} \left(m_W^2 W^2 + \frac{1}{2} m_Z^2 Z^2 \right) h . \quad (3)$$

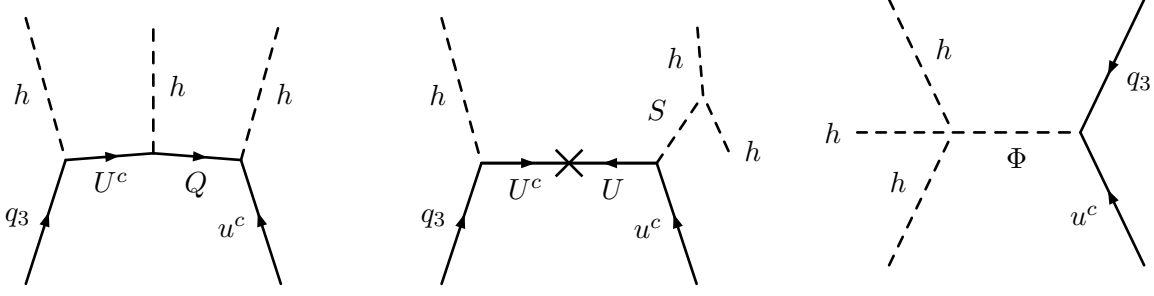


FIG. 1: Possible tree level Feynman diagrams associated to the dimension 6 operator in Eq. 1. On the left, the new particles contributing to the top Yukawa are two top quark partners Q and U (model 1), in the middle, one top quark partner U and one singlet S (model 2), and on the right, a new electroweakly charged scalar Φ (model 3).

In the SM, $\kappa_t = \kappa_V = 1$. The 2σ bounds on these parameters from the ATLAS $h \rightarrow \gamma\gamma$ [25], $h \rightarrow WW \rightarrow 2l2\nu$ [33] and $h \rightarrow ZZ \rightarrow 4l$ [34] are shown in Fig. 2. The allowed regions in the (κ_t, κ_V) space are defined by the intersection of the three bounds mentioned above and are therefore larger than the regions we would find using a full statistical analysis. As can be seen from Fig. 2 the non-SM region of top Yukawa still allowed by the data is $-1 \lesssim \kappa_t \lesssim -0.8$.

2. FERMIONIC TOP PARTNERS

The effective operator shown in Eq. 1 can be generated by introducing fermionic top partners. The diagrams in Fig. 1 show two classes of minimal models. The corresponding new particles could be either a pair of top partners Q and U , or one top partner Q or U and a scalar η with charge $(1, 0)$ or $(3, 0)$ under $SU(2) \times U(1)$. Here, we focus on extensions of the SM with either two top partners or one top partner and a scalar singlet.

Models studied in this section involve light Dirac top partners and are therefore strongly constrained by the corresponding ATLAS [35] and CMS [36] searches. The top partner production cross section is dominated by pair production through gluons and is therefore model independent. Branching ratios associated to the three top partner decay modes $Q, U \rightarrow Wb, tH$ and tZ depend however on the $SU(2)$ quantum numbers and Yukawa

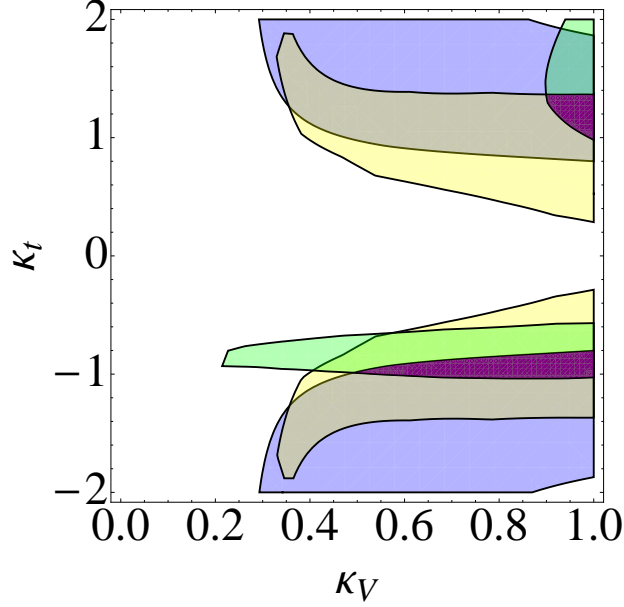


FIG. 2: 2σ bounds on κ_t and κ_V from the ATLAS $\rightarrow \gamma\gamma$ (green), $h \rightarrow WW \rightarrow 2l2\nu$ (yellow) and $h \rightarrow ZZ \rightarrow 4l$ (blue) searches. The intersection of all these bounds is in purple.

couplings of the top partners. Both CMS and ATLAS searches accommodate all the corresponding possibilities by giving bounds on the top partner mass for all possible combinations of the three branching ratios. Throughout this section, we use the loosest possible bound on the top quark mass, which is around 650 GeV.

2.1. Two top partners

The effective operator shown in Eq. 1 can be generated by extending the SM with two vector-like fermions (Q, Q^c) and (U, U^c) whose quantum numbers are:

$$Q \sim (3, 2, \frac{1}{6}) \quad Q^c \sim (\bar{3}, 2, -\frac{1}{6}) \quad U \sim (3, 1, \frac{2}{3}) \quad U^c \sim (\bar{3}, 1, -\frac{2}{3}). \quad (4)$$

Similar fields can be found in Little Higgs [37–39] and Randall-Sundrum [40] models. The corresponding Lagrangian is

$$\mathcal{L}_{\text{int}} = y_0 h q_3 u^c + y_1 h q_3 U^c - y_2 h Q U^c + y_3 h Q u^c + M_1 U U^c + M_2 Q Q^c \quad (5)$$

Since this model involves two new fields, only two of the three new Yukawa couplings – y_1 , y_2 and y_3 – can be made positive by phase redefinition. Here, we define y_0 , y_1 and y_3 to be positive while the sign of y_2 remains free. With the parameterization of Eq. 5, in order to get a negative Higgs coupling to the top quark mass eigenstate, y_2 will then have to be positive. The corresponding mass matrix is

$$M = \begin{pmatrix} \frac{y_0 v}{\sqrt{2}} & \frac{y_1 v}{\sqrt{2}} & 0 \\ 0 & M_1 & 0 \\ \frac{y_3 v}{\sqrt{2}} & \frac{-y_2 v}{\sqrt{2}} & M_2 \end{pmatrix} \quad (6)$$

This new model involves three states mixing with each other and has six new parameters. However, viable models need to obey the following four constraints:

- the lightest mass eigenstate has mass m_t
- the other top quark partners have to be heavier than the lower mass bounds set by the ATLAS [35] and CMS [36] searches.
- the Yukawa couplings have to remain perturbative up to about 10 TeV
- $-1 < \kappa_t < -0.8$ where κ_t is the ratio of the top Yukawa coupling over its SM value.

For small mixing angles, satisfying this last constraint requires large Yukawa couplings, which are likely to lead to low scale Landau poles. As we will see, even if we ignore the second constraint there is no way to satisfy the other requirements.

The RGEs for the top Yukawa couplings [41] are shown in Appendix D. When all the Yukawa couplings are equal, the system exhibits a $\mathbb{Z}_2 \times \mathbb{Z}_2$ symmetry which allows to show that the configuration for which the perturbativity bounds are the loosest is the one with

$$|y_0| = |y_1| = |y_2| = |y_3| = y , \quad (7)$$

for which Landau poles below 10 TeV are avoided if and only if $y \lesssim 1.06$. Fig. 3 shows the range of possible values for y_{eff} in function of y for positive y and $M_1, M_2 > 100$ GeV. The minimum y_{eff} that can be reached here is

$$y_{\text{eff}} \sim 0.9 . \quad (8)$$

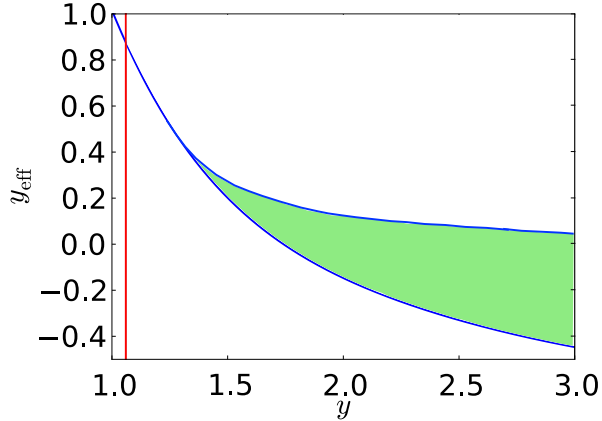


FIG. 3: Range of y_{eff} vs y for $y = y_0 = y_1 = y_2 = y_3$ and $M_1, M_2 > 100 \text{ GeV}$ (green). The red line shows the maximal value of y for which there are no Landau poles below 10 TeV.

Models not satisfying Eq. 7 will in general be more constrained by the perturbativity requirement and are therefore not expected to give significantly better results than the simple model outlined here. To show this, we expand away from the \mathbb{Z}_2 limit by scanning over the full 5D parameter space. As in the previous section, the Yukawa coupling RGEs (shown in Appendix D) forbid Yukawa couplings greater than 1.06.

We scan over $[-2, 0]$ for y_2 and $[0, 2]$ for y_1 and y_3 with a step size of 0.05. M_1 and M_2 are scanned over the range $[400 \text{ GeV}, 1000 \text{ GeV}]$ with a step size of 100 GeV. y_0 is fixed by requiring the lightest mass eigenstate to be the top quark. Requiring the heavy top quarks to be heavier than 650 GeV and the Yukawa couplings to remain perturbative up to 10 TeV, the minimum y_{eff} that can be reached is

$$y_{\text{eff}} \sim 0.73 . \quad (9)$$

Since the top Yukawa coupling y_{eff} is a well-behaved function of the different parameters scanned over and the step size is small, the existence of regions of parameter space with a Yukawa coupling close to minus one and no low scale Landau poles is highly unlikely.

2.2. Top partner plus singlet

Extending the SM with a vector-like top quark partner Q ($SU(2)$ doublet) or U ($SU(2)$ singlet) and a scalar singlet S leads to the second diagram of Fig. 1. The Lagrangians for these simple models are

$$\mathcal{L}_{int} = y_0 h q_3 u^c + y_1 S U u^c + y_2 H q_3 U^c + \lambda' S h^\dagger h + M U U^c + \frac{1}{2} M_S^2 S^2 \quad (10)$$

$$\mathcal{L}_{int} = y_0 h q_3 u^c + y_1 S q_3 Q^c + y_2 H Q u^c + \lambda' S h^\dagger h + M Q Q^c + \frac{1}{2} M_S^2 S^2 \quad (11)$$

where q , u^c and H are the interaction eigenstates corresponding to the left and right-handed top quarks and the Higgs doublet respectively. In what follows, we also choose S to be a complex scalar. This choice affects only the RGEs, which would lead to tighter bounds on the values of the Yukawa couplings if S is a real scalar. If the S does not get a vev, the fermion mass matrix is

$$M_F = \begin{pmatrix} \frac{y_0 v}{\sqrt{2}} & \frac{y_2 v}{\sqrt{2}} \\ 0 & M \end{pmatrix} \quad (12)$$

The mass of the heavy top partner can then be expressed as

$$m_T = m_t \frac{y_0}{y_{SM}} \sqrt{1 + \frac{y_2^2}{y_0^2 - y_{SM}^2}} \quad (13)$$

The left and right-handed mass eigenstates are characterised by the mixing angles β and α respectively, given by

$$\sin \alpha = \frac{1}{\sqrt{1 + z^2(x^2 - 1)}}, \quad \sin \beta = \frac{x}{\sqrt{1 + z^2(x^2 - 1)}}, \quad (14)$$

where

$$x = \frac{y_{SM}}{y_0} \frac{m_T}{m_t} > 1, \quad z = \frac{y_0}{\sqrt{y_0^2 - y_{SM}^2}} > 1. \quad (15)$$

EWSB induces a mixing between h^0 and S , with mixing angle θ . Diagonalizing the scalar mass matrix gives two mass eigenstates: h_1^0 (the 125 GeV Higgs) and h_2^0 , defined by

$$h_1^0 = \cos \theta h^0 - \sin \theta S \quad h_2^0 = \sin \theta h^0 + \cos \theta S. \quad (16)$$

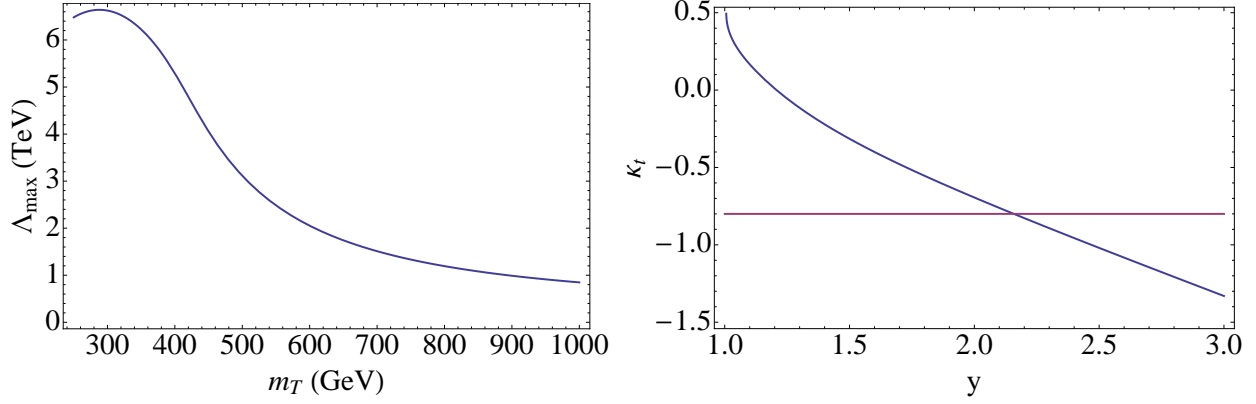


FIG. 4: Maximum possible scale for the Landau poles (in TeV) in function of m_T (GeV) for $\kappa_t = -0.8$ and $\kappa_V = 0.5$ (left). κ_t in function of $y = y_0 = y_1 = y_2$ (right).

The coupling of h to the top quark mass eigenstate, y_{eff} , is then given by

$$y_{\text{eff}} = y_0 \cos \theta \cos \beta \cos \alpha + y_1 \sin \theta \sin \beta \cos \alpha + y_2 \cos \theta \cos \beta \sin \alpha \quad (17)$$

Using Eqs 17 and expressing α and β in function of y , y_1 and m_T , we get

$$|y_1| = \frac{(y_{\text{SM}}^2 m_T^2 - y_0^2 m_t^2)(2y_0^2 - y_{\text{SM}}^2) \cos \theta - \kappa_t y_{\text{SM}}^2 y_0^2 (m_T^2 - m_t^2)}{m_T y_0^2 \sin \theta \sqrt{(y_0^2 - y_{\text{SM}}^2) \left(\frac{m_T^2}{y_0^2} - \frac{m_t^2}{y_{\text{SM}}^2} \right)}} \quad (18)$$

The limits on κ_t , κ_V from the ATLAS Higgs searches [23] for this model are shown in Fig. 2. For negative κ_t , the allowed region is $\kappa_V \geq 0.5$ and $-1 \leq \kappa_t \leq -0.8$. The case of $\kappa_V = 0.5$ and $\kappa_t = -0.8$ yields the lowest possible values of $|y_1|$ for given y_0 , m_T . For this choice of parameters and using the RGEs shown in App. C, Fig. 4 shows the maximum possible energy scales Λ that can be reached in function of m_T . As shown in Sec. 1.1, the lowest possible bound on m_T from the ATLAS and CMS searches [36, 42] is around 650 GeV, which would correspond to Landau poles below 2 TeV. Models where the top Yukawa coupling is driven negative by introducing one Dirac top partner and one scalar singlet can therefore be excluded.

3. INTRODUCING ADDITIONAL SCALARS

The effective operator shown in Eq. 2 can be generated by introducing new scalar fields as shown in the rightmost diagram of Fig. 1. Since these scalars have to couple both to the Higgs and to the top quarks, they have to be $SU(2)$ doublets. Since the corresponding models do not involve light new colored particles, they are expected to be less constrained than the models involving top partners studied in the previous section. A minimal scenario which could lead to a negative top Yukawa coupling would then be a two Higgs doublet model [30–32] in which the second Higgs interaction eigenstate has a large negative Yukawa coupling to the top quark.

3.1. A minimal model

The minimal Lagrangian needed to obtain the operator in Eq. 2 is

$$\mathcal{L} = (yh_1 + y'h_2)q_3u_3^c - \lambda(|h_1|^2 - v^2/2)^2 - \frac{1}{2}m_{h_2}^2|h_2|^2 - \lambda'h_2^\dagger h_1(|h_1|^2 - v^2/2) + \text{h.c.} \quad (19)$$

In this preliminary study, many terms usually encountered in two Higgs doublet models are set to zero for simplicity. We show later that introducing them does not modify our conclusions. One benefit of this simple model is that the new interaction eigenstate h_2 does not get a vev. The interaction eigenstates h_1 and h_2 are then of the form

$$h_1 = \begin{pmatrix} G^\pm \\ \frac{v + h_1^0 + iG^0}{\sqrt{2}} \end{pmatrix} \quad h_2 = \begin{pmatrix} H^\pm \\ \frac{h_2^0 + iA^0}{\sqrt{2}} \end{pmatrix} \quad (20)$$

The λ' quartic term induces a mixing between h_1^0 and h_2^0 with a mixing angle θ . In what follows, we name the 125 GeV mass eigenstate h^0 and the other mass eigenstate H^0 . Since the concept of a negative top Yukawa coupling is ambiguous if h^0 and H^0 are indistinguishable, we consider only the case where the mass difference between the two Higgses is greater than 3 GeV, the mass resolution of ATLAS and CMS.

The interaction Lagrangian for the 125 GeV Higgs mass eigenstate h^0 is

$$\mathcal{L} = \frac{m_t \cos \theta}{\sqrt{2}v} (1 + \tan \theta r) h^0 t t^c + (m_W^2 W^2 + m_Z^2 Z^2 / 2) h^0 \cos \theta$$

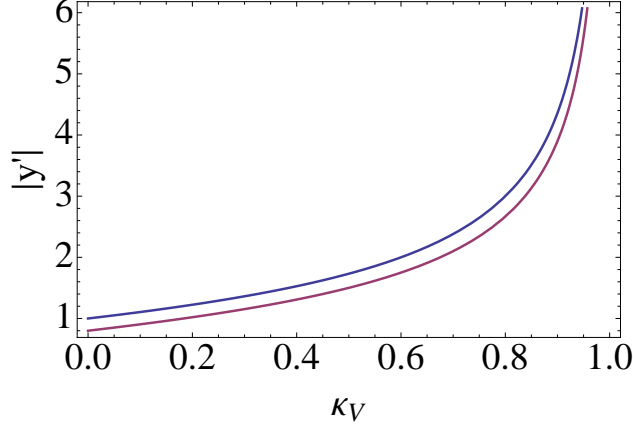


FIG. 5: $|y'|$ in function of κ_V for $\kappa_t = -1$ (blue) and $\kappa_t = -0.8$ (red)

with $r = y'/y$. The couplings y and y' can be rewritten in function of κ_t and κ_V to give

$$y = y_{SM} \quad y' = y_{SM} \frac{\kappa_t - \kappa_V}{\sqrt{1 - \kappa_V^2}} \quad (21)$$

Fig. 5 shows the dependance of y' on κ_V for $\kappa_t = -1, -0.8$. From this, we see that for $\kappa_V \gtrsim 0.5$ the Yukawa couplings are likely to become non perturbative at the TeV scale. Keeping y' low will then require a large mixing angle between the two Higgses, leading to a significant suppression of the Higgs detection rates for vector boson fusion and associated production. This minimal two-Higgs model will then be strongly constrained by the current Higgs results.

The RGEs for y and y' are

$$16\pi^2 \frac{dy}{d\log \mu} = \frac{9}{2} (y^2 + y'^2) y - 8y g_s^2 \quad (22)$$

$$16\pi^2 \frac{dy'}{d\log \mu} = \frac{9}{2} (y^2 + y'^2) y' - 8y' g_s^2 \quad (23)$$

where g_s is the strong coupling and the electroweak interactions have been neglected. As can be seen in Eq. 21, the value of y' for $\mu = m_{\text{top}}$ strongly depends on κ_t and κ_V . The left-hand side of Fig. 6 shows the values of κ_t and κ_V for which the Yukawa couplings become non perturbative only above 10 TeV as well as the intersection of the ATLAS bounds shown in Fig. 2.

Since the ATLAS bounds tend to favor relatively large values of κ_V , they are in tension with the perturbativity bounds. The intersection of all the allowed (κ_t, κ_V) regions leaves

open only a small negative κ_t region of the parameter space. Since the allowed regions have been obtained by intersecting several two sigma bounds, a more rigorous statistical analysis might exclude the remaining negative top Yukawa region at two sigma. In what follows, however, we are going to assume that the two regions shown in Fig. 6 are still allowed by the ATLAS results.

The allowed region of the (κ_t, κ_V) space corresponding to negative values of the top Yukawa coupling is extremely small and centered around

$$\kappa_t = -0.9 \quad \kappa_V = 0.5 \quad (24)$$

which corresponds to a factor of four suppression of the Higgs production cross section for vector boson fusion and associated production. The detection rate associated to the $W/Zh \rightarrow b\bar{b}$ searches will therefore be drastically reduced compared to its expected SM value. Although the observed signal strengths for this process in ATLAS and CMS are consistent with zero [43, 44], the bounds from the combined CDF and D0 analysis at the Tevatron [26] are tighter and might lead to further constraints on κ_V .

The combination of the CDF and D0 results at the Tevatron shows a 3.5 sigma excess in the $W/Zh \rightarrow b\bar{b}$ channel [26]. Such an excess allows to exclude the null hypothesis at two sigma and therefore, allows to set a two-sigma lower bound on κ_V . Since the only decay widths that are not proportional to κ_V are for $h \rightarrow \gamma\gamma$ and $h \rightarrow gg$ and are subdominant, therefore, the Higgs branching ratios are approximately unaltered. The signal strength associated to our model would then be

$$\mu = \kappa_V^2 \frac{\text{Br}(h \rightarrow b\bar{b})}{\text{Br}_{\text{SM}}(h \rightarrow b\bar{b})} \sim \kappa_V^2 \quad (25)$$

which leads to

$$\kappa_V \geq \frac{1}{\sqrt{3}} \quad (26)$$

The exact two-sigma bound in the (κ_t, κ_V) space is shown in the right-hand side of Fig. 6, superimposed on the bounds previously obtained from the perturbativity requirement and from the ATLAS Higgs searches. The Tevatron bound is found to exclude the region of parameter space still allowed by these previous limits.

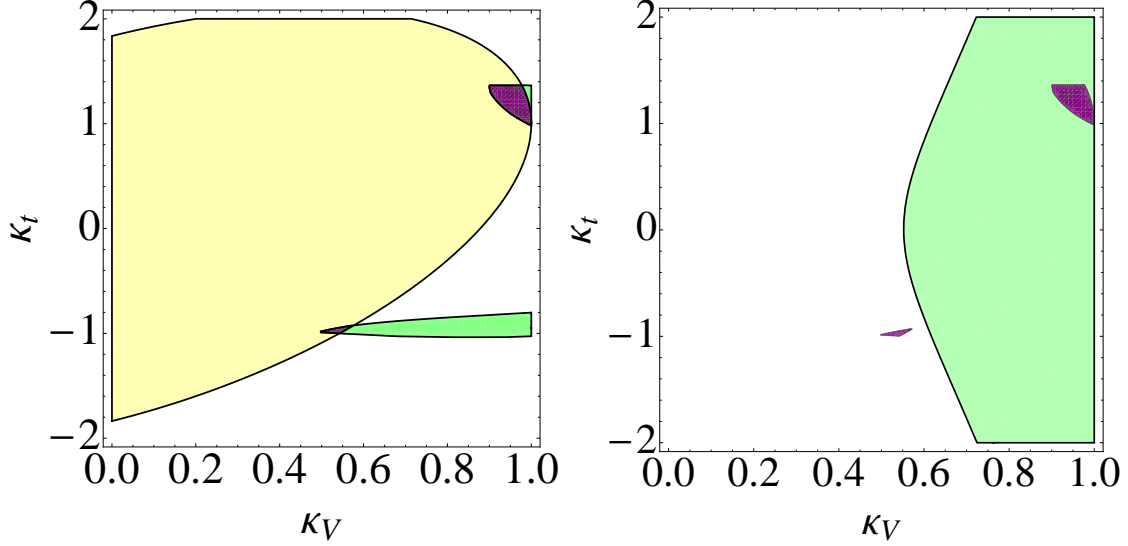


FIG. 6: Left: Values of κ_t , κ_V for which the top Yukawa couplings become perturbative only above 10 TeV (yellow) and intersection of the regions allowed by the ATLAS $h \rightarrow \gamma\gamma$ [25], $h \rightarrow WW \rightarrow 2l2\nu$ [33] and $ZZ \rightarrow 4l$ [34] searches (light green). The intersection of all the regions is shown in purple. Right: Intersection of the ATLAS and perturbativity bounds (purple) and region allowed by the combined CDF and D0 analysis for $WH \rightarrow b\bar{b}$ [26] (green).

A minimal model with two Higgses as the one shown in Eq. 19, with only one of the Higgses getting a vev, cannot explain the negative values of the top Yukawa couplings allowed by ATLAS. One of the main issues of such a model is that, in order for the top Yukawa couplings to remain perturbative up to a high scale, the mixing angle between the two Higgses needs to be large. Such a large mixing results in a significant suppression of the Higgs trilinear coupling to vector bosons, which is incompatible with the current LHC [23] and Tevatron [26] Higgs results. Since the different allowed regions are close to each other, we further explore alternate more elaborate models to check how robust our conclusion is. Ultimately, obtaining a model which survives the ATLAS and Tevatron bounds will require adding novel Higgses, as will be shown in Sec. 3.4.

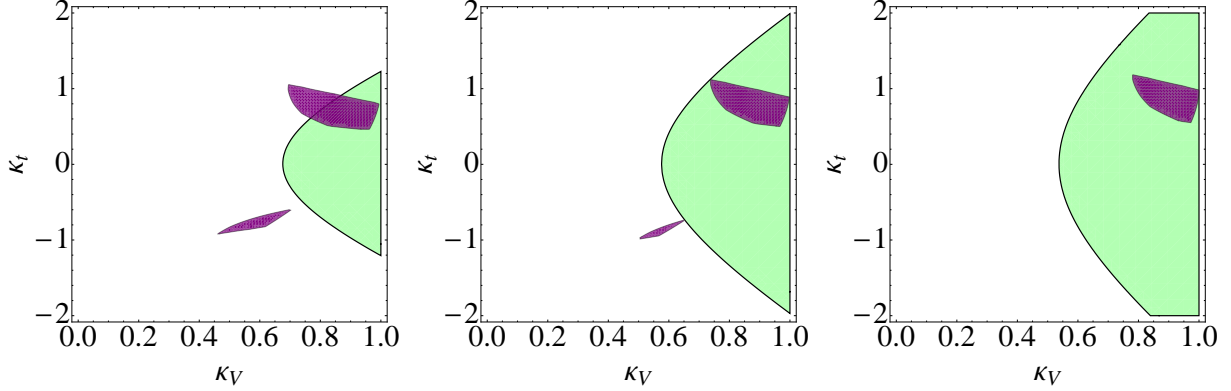


FIG. 7: ATLAS and perturbativity bounds (purple) and Tevatron bounds (green) on κ_t and κ_V with $\kappa_b = 0.4$ (left), $\kappa_b = 0.5$ (center) and $\kappa_b = 0.6$ (right). $\kappa_b \sim 0.5$ is where the different bounds are the closest to each other. .

3.2. Possible extensions of the minimal model

The minimal model described by Eq. 19 excludes any large deviation from the SM top Yukawa couplings. In what follows, we argue that introducing new Higgs couplings as well as choosing more general parameterizations does not open new negative top Yukawa regions.

The minimal model in Eq. 19 had two free parameters that modified the Higgs couplings at tree level: κ_t and κ_V . Introducing a coupling of h_2 to down-type quarks would allow to freely modify the coupling of the Higgs to bottom quarks and have a third handle, κ_b , defined the same way as κ_t . If $\kappa_V = \cos\theta$ as before, the perturbativity bounds shown in Fig. 6 will remain the same. As shown in Fig. 7, increasing κ_b would lead to weaker Tevatron bounds but also to a uniform suppression of the Higgs detection rates in the different ATLAS Higgs detection channels, due to the lower corresponding branching ratios. Decreasing κ_b allows larger detection rates in all the ATLAS channels [25, 33, 34] but leads to even tighter Tevatron bounds [26]. Both configurations therefore exclude the negative κ_t region at two sigma.

It is worth noting that models where both Higgses get a vev can be treated as a subset of the free κ_b case described above. Indeed, we can now redefine κ_V as

$$\kappa_V = \cos(\theta - \beta) , \quad (27)$$

where β is the mixing angle between the two vevs such that $\beta = 0$ corresponds to the minimal model studied in Sec. 3.1. The only couplings which will be modified in the (κ_t, κ_V) space will be the couplings of the Higgs to fermions other than the top, for which we can define

$$\kappa_f = \cos \theta \cos \beta \quad (28)$$

In practice, since the ATLAS and CMS bounds on the Higgs couplings to fermions other than the top and bottom quark are extremely loose [35, 43–47], introducing a non zero β angle is equivalent to introducing a κ_b such that

$$\kappa_b = \begin{cases} \kappa_V \cos \beta + \sqrt{1 - \kappa_V} \sin \beta & \text{for } \theta < \beta \\ \kappa_V \cos \beta - \sqrt{1 - \kappa_V} \sin \beta & \text{for } \theta > \beta \end{cases} \quad (29)$$

Models where both Higgses get a vev will then not allow for negative values of the top Yukawa coupling.

As shown in the previous section, the main source of tension between the different Higgs results for a negative top Yukawa is the high suppression of the Higgs coupling to vector bosons. As shown above, increasing the corresponding branching ratios by suppressing the Higgs coupling to bottom quarks leads to a conflict with the Tevatron bounds. These results, however, were obtained for models with only two Higgs doublets. The following sections study how the collider and perturbativity bounds evolve when additional scalars are introduced.

3.3. Arbitrary number of Higgs doublets

The conclusions of the previous sections were valid for two Higgs doublets. Here, we argue that they can be extended to the case of an arbitrary number of $SU(2)$ doublets mixing with each other. In particular, we show that adding Higgs doublets makes the perturbativity bounds tighter.

The RGEs for the Yukawa couplings [41] remain similar to the ones in Eq. 23

$$16\pi^2 \frac{d \log y_i}{dt} = \frac{9}{2} \sum_{k=1 \dots N} y_k^2 - 8g_s^2 \quad (30)$$

Since the right hand side of Eq. 30 is the same for all couplings, the ratios of the Yukawa couplings do not depend on the energy scale. Writing $y_i(t) = y_1(t)K_i$ gives

$$16\pi^2 \frac{dy_1}{dt} = \frac{9}{2} y_1^3 \sum_{k=1\dots N} K_k^2 - 8y_1 g_s^2 \quad (31)$$

Close to the Landau pole, the y_1^3 term will dominate and the RGE can be solved analytically. The position of the Landau pole, μ_L , will be given by

$$\sum_{k=1\dots N} y_k^2 \log \frac{\mu_L}{\mu_0} = \frac{16\pi^2}{9} \quad (32)$$

Requiring no Landau poles below 10 TeV leads to the following constraint on the sum of the squares of the Yukawa couplings

$$\sum_{k=1\dots N} y_k^2 \leq 4.33 \quad (33)$$

which can be rewritten as

$$|\vec{y}|^2 \leq 4.33 \quad (34)$$

by defining $\vec{y} = (y_1, \dots, y_N)$. Similarly, defining the vev as $\vec{v} = (v_1, \dots, v_N)$ and the Higgs mass eigenstates as $\vec{H} = (H_1, \dots, H_N)$ in the orthonormal basis defined by the Higgs interaction eigenstates, the constraints on the initial values of the top Yukawas are

$$\vec{y} \cdot \hat{v} = y_{SM}, \quad \vec{y} \cdot \hat{H} = \kappa_t y_{SM} \quad (35)$$

Redefining \hat{H} and \vec{y} as

$$\hat{H} = \cos \theta \hat{v} + \sin \theta \hat{H}_\perp, \quad \vec{y} = y_{SM} \hat{v} + \vec{y}_\perp \quad (36)$$

Eq. 35 becomes

$$\vec{y}_\perp \cdot \hat{H}_\perp = y_{SM} \frac{\kappa_t - \cos \theta}{\sin \theta} \quad (37)$$

Thus,

$$|\vec{y}_\perp| \geq y_{SM} \frac{|\kappa_t - \cos \theta|}{\sin \theta} \quad (38)$$

So we finally get

$$|\vec{y}|^2 \geq \frac{1 + \kappa_t^2 - 2\kappa_t \cos \theta}{\sin^2 \theta} \quad (39)$$

Writing the vector boson couplings after symmetry breaking gives

$$\kappa_V = \cos \theta \quad (40)$$

and finally, we get

$$|\vec{y}|^2 \geq \frac{1 + \kappa_t^2 - 2\kappa_t \kappa_V}{1 - \kappa_V^2} \quad (41)$$

Combining this result with Eq. 34, we see that a *necessary* condition to avoid Landau poles below 10 TeV is

$$\frac{1 + \kappa_t^2 - 2\kappa_t \kappa_V}{1 - \kappa_V^2} \leq 4.33 \quad (42)$$

The bound in Eq. 41 is saturated if there are two Higgses. The bounds on κ_t and κ_V associated to Eq. 42 are then the ones shown in Fig. 6. For more than two Higgses, the bounds in Eq. 41 are not saturated and the associated bounds on κ_t , κ_V are more restrictive than the ones shown in Fig. 6. So if negative values of κ_t are not allowed for two Higgs bosons, they are also not allowed for any larger number of Higgs bosons. Note that this result also applies when all Higgs scalars get arbitrary vevs.

SM extensions with an arbitrary number of Higgs doublets and a negative top Yukawa coupling are then either excluded by ATLAS and the Tevatron, or have low scale Landau poles. The tension between the different collider bounds is caused by the large mixing angle suppression of the Higgs coupling to vector bosons required by the perturbativity bounds. Viable extensions of the minimal model studied in Sec. 3.1 should then have κ_V close to one.

3.4. New representations of $SU(2)$

The 125 GeV Higgs boson observed in the LHC couples to vector bosons and fermions while the second Higgs boson introduced in our model has to couple at least to the top quark to drive the top Yukawa negative. Therefore, both Higgses have to be $SU(2)$ doublets,

and their couplings to gauge bosons are then fully determined. The only way to increase κ_V would then be to mix the two Higgses with scalars embedded in higher representations of $SU(2)$ [48–52]. In what follows, we focus on representations of isospin less than two, so triplet scalars.

Introducing a single scalar triplet, Φ , is the most straightforward way of extending our model [48–50, 53]. This triplet gets a vev, v_Δ , and includes a neutral scalar particle ϕ^0 , which mixes with the two Higgses. The mixing angles and the vevs are defined such that

$$h^0 = h_1^0 \cos \alpha \cos \theta + h_2^0 \cos \alpha \sin \theta + \phi^0 \cos \gamma \quad (43)$$

$$v_\Delta = v \sin \alpha \quad (44)$$

Defining β as the angle between the vevs of the two Higgs doublets, the ratios of the 125 GeV Higgs couplings to gauge bosons over their SM values are

$$\kappa_{hWW} = \cos \alpha \sin \gamma \cos(\beta - \theta) + \sqrt{2(2 - Y^2)} \sin \alpha \cos \gamma \quad (45)$$

$$\kappa_{hZZ} = \frac{\cos \alpha \sin \gamma \cos(\beta - \theta) + 4Y^2 \sin \alpha \cos \gamma}{\sqrt{\cos^2 \alpha + 4Y^2 \cos^2 \alpha}} \quad (46)$$

where Y is the hypercharge of the Higgs triplet. The couplings of the 125 GeV Higgs to fermions other than the top are then defined by

$$\kappa_{hff} = \frac{\sin \gamma \cos \theta}{\cos \alpha \cos \beta} \quad (47)$$

For $Y \leq 1$, a new Higgs triplet could then in principle increase κ_V without leading to low scale Landau poles. However, since such triplet models violate custodial symmetry, v_Δ is strongly constrained to be [54]:

$$v_\Delta < 3 \text{ GeV} \quad (48)$$

which leads to

$$\sin \alpha < 0.01 \quad (49)$$

and the resulting increase in κ_V will be negligible.

In order to get a significant increase in κ_V , the additional scalars have to come in complete $SU(2)_C$ multiplets. This can be realized by introducing one $Y = 1$ complex triplet and one $Y = 0$ triplet, which can be rearranged to form a $(3, \bar{3})$ of $SU(2)_L \times SU(2)_R$:

$$\Delta = \begin{pmatrix} \chi^{0*} & \xi^+ & \chi^{++} \\ \chi^- & \xi^0 & \xi^+ \\ \chi^{--} & \xi^- & \chi^0 \end{pmatrix} \quad (50)$$

This model can be viewed as a simple extension of the Georgi-Machacek model [52], with one additional Higgs doublet. In order for custodial symmetry to be enforced, the triplet vevs have to be diagonal

$$v_\chi = v_\xi \quad (51)$$

This time, the mixing angle α is defined such that

$$v_\chi = \frac{v}{\sqrt{8}} \sin \alpha \quad (52)$$

and the 125 GeV Higgs couplings become

$$\kappa_{hWW} = \kappa_{hZZ} = \kappa_V = \cos \alpha \sin \gamma \cos(\beta - \theta) + \sqrt{\frac{8}{3}} \sin \alpha \cos \gamma \quad (53)$$

$$\kappa_{hff} = \frac{\sin \gamma \cos \theta}{\cos \alpha \cos \beta} \quad (54)$$

Since this model does not violate custodial symmetry at tree level, the triplet vev v_χ can now go up to about 100 GeV. Such a large vev allows to alleviate the tension between the ATLAS and Tevatron bounds while avoiding low scale Landau poles.

Since this model respects the custodial symmetry $SU(2)_C$ [55], the nine Higgs fields in Δ , can be rearranged in full $SU(2)_C$ multiplets – a five-plet H_5 , a triplet \tilde{H}_3 and a singlet \tilde{H}_1 – using

$$\mathbf{9} = \mathbf{5} \oplus \mathbf{3} \oplus \mathbf{1} \quad (55)$$

Besides the 125 GeV Higgs h^0 , this model then implies the existence of 12 new scalars:

- 3 Goldstone bosons which are eaten by the W and Z bosons

- 3 charged Higgses H_1^\pm , H_2^\pm and H_3^\pm
- one doubly charged Higgs H_3^{++}
- 3 pseudoscalar Higgses A_1^0 , A_2^0 and A_3^0
- 2 CP-even Higgses H_1^0 and H_2^0

Fig. 8 shows the ATLAS, Tevatron and perturbativity bounds for $\alpha = 0.52$, $\beta = 0.20$ and $\gamma = 1.12$ in function of κ_t and $\cos(\theta - \beta)$. Although the tension between the different ATLAS [25, 33, 34] and Tevatron [26] searches is alleviated in this new model, the allowed region of parameter space remains limited.

The Georgi-Machacek model [52] with one additional Higgs doublet allows us to reconcile the different collider and perturbativity bounds on the 125 GeV Higgs boson. It predicts, however, a large number of new particles which are within the reach of the current LHC searches.

3.4.1. The need for alternate Higgs decay modes

The Georgi-Machacek model studied here predicts the existence of three neutral CP-even Higgs bosons: a 125 GeV Higgs analogous to the one observed in ATLAS and CMS, h^0 , and two new scalars H_1^0 and H_2^0 , whose masses will be constrained by the current ATLAS and CMS Higgs results. For Higgses heavier than about 140 GeV, the most sensitive search is the CMS $H \rightarrow ZZ \rightarrow 4l$ search [56], which constrains the detection rate of heavy Higgses to be no larger than about 30% of the SM one. Lighter Higgs bosons are constrained by the ATLAS $H \rightarrow \gamma\gamma$ search [25], and, in most of the mass range, their detection rate in this channel should be no larger than about half the SM one. Here again, we choose to leave apart the region where the two Higgses are nearly degenerate.

Although both ATLAS and CMS require H_1^0 and H_2^0 to have suppressed couplings, generating a large negative Yukawa coupling requires one of the Higgs interaction eigenstates to have a large coupling y' to the top, as shown in Fig. 5 and Eq. 21. In the minimal model

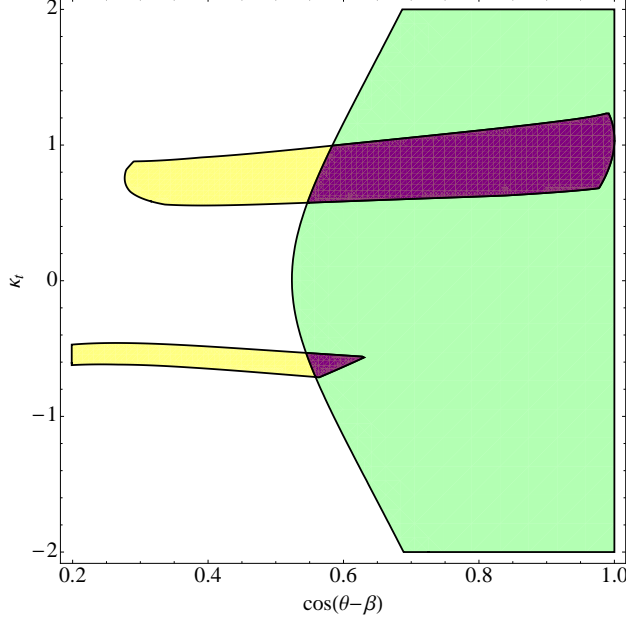


FIG. 8: Perturbativity bounds and ATLAS $h \rightarrow WW \rightarrow ll\nu\nu$ [33], $h \rightarrow \gamma\gamma$ [25] and $h \rightarrow ZZ \rightarrow 4l$ [34] bounds (yellow) in the $(\cos(\theta - \beta), \kappa_t)$ space. The Tevatron [26] bound is shown in green. The intersection of all the different bounds is shown in purple. The model is a Georgi-Machacek [52] model with two Higgs doublets instead of one and $\alpha = 0.52$, $\beta = 0.2$ and $\gamma = 1.12$.

shown in Sec. 3.1, this large y' leads to an enhanced coupling of the second Higgs mass eigenstate to the top quark

$$\frac{y_{Ht\bar{t}}}{y_{SM}} = \frac{\kappa_t \kappa_V - 1}{\sqrt{1 - \kappa_V^2}} > 1 \text{ for } \kappa_t < 0. \quad (56)$$

This enhanced coupling to the top quark leads to a larger production rate of the second Higgs boson through gluon fusion. Here, for $\kappa_t = -1$ and $\kappa_V = 0.5$, we would have

$$\frac{\sigma_{GGF}}{\sigma_{GGF}^{SM}} = \left(\frac{\kappa_t \kappa_V - 1}{\sqrt{1 - \kappa_V^2}} \right)^2 = 3. \quad (57)$$

In order for H_1^0 and H_2^0 to be within the current ATLAS and CMS bounds, the branching ratios in the channels of interest should then be reduced by a factor of about 10. In order to our models to be viable, the new Higgs bosons must then couple to particles other than SM fermions and vector bosons.

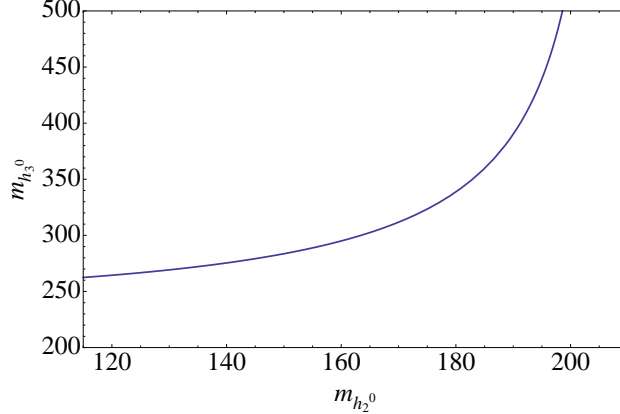


FIG. 9: Mass of ϕ^0 in function of m_H for $\alpha = 0.52$, $\gamma = 1.12$, $\beta = 0.2$ and $\kappa_V = 0.57$.

The modified Georgi-Machacek model described here predicts the existence of two new Higgs mass eigenstates, H_1^0 and H_2^0 . In order to drive the top Yukawa coupling negative without significantly suppressing the 125 GeV Higgs coupling to vector bosons, the mixing between the three neutral Higgs interaction eigenstates needs to be large. This large mixing constrains the lightest new mass eigenstate, H_1^0 , to be lighter than 200 GeV, as shown in Fig. 9.

Having large mixing angles between the neutral CP-even Higgses also means that all three mass eigenstates h^0 , H_1^0 and H_2^0 will have sizeable couplings to the top quark. The production cross sections of H_1^0 and H_2^0 through gluon fusion will then be comparable to the SM ones. Since these new Higgses have not been observed, they must have non SM decay modes. Although H_2^0 , if heavy enough, can decay to two Higgs bosons, this decay mode is forbidden for H_1^0 , which has to be lighter than 200 GeV. H_1^0 then needs to have alternate decay modes. In what follows, we assume that H_1^0 and H_2^0 can decay to invisible particles. Scenarios involving similar interactions have been studied in models with Higgs-portal dark matter [57–66].

Coupling the Higgs interaction eigenstates to invisible particles can induce new decay modes for the 125 GeV Higgs boson. These new invisible decay modes would lead to suppressed detection rates for the 125 GeV Higgs boson in all the different detection channels. Our previous two Higgs doublet model, however, suffered from a suppressed coupling of the

125 GeV Higgs to vector bosons, which lead to a strong suppression of the detection rate in the $H \rightarrow ZZ \rightarrow 4l$ [34] and the $H \rightarrow WW \rightarrow 2l2\nu$ [33] channels. Since, as shown in Fig. 8, introducing new Higgs triplets barely compensates for this suppression, opening new invisible decay channels for the 125 GeV Higgs would lead us to the same issues as the ones considered in Sec. 3.1. The masses of a new invisible particle S coupling to the neutral Higgs bosons of our model would then be constrained by:

$$\frac{m_h}{2} \sim 63 \text{ GeV} \lesssim m_S \lesssim \frac{m_{\phi^0}}{2} \lesssim 100 \text{ GeV}. \quad (58)$$

In what follows, we assume that S is a SM singlet and couples to the Higgs interaction eigenstates through

$$\mathcal{L} \supset \lambda_1 h_1^\dagger h_1 S^\dagger S + \lambda_2 h_2^\dagger h_2 S^\dagger S + \lambda_3 \Delta^\dagger \Delta S^\dagger S \quad (59)$$

3.4.2. A possible model

This section studies one possible benchmark model satisfying all the current constraints from collider searches and perturbativity requirements described in Sec. 3.1. The mixing angles we choose here are the same as the ones in Fig. 8:

$$\alpha = 0.52 \quad \beta = 0.2 \quad \theta = 1.16 \quad \gamma = 1.12 \quad (60)$$

For this choice of angles and

$$\kappa_t = -0.55 \quad \kappa_V = 0.57 \quad (61)$$

one possible spectrum is

$$m_{H_1^\pm} = m_{A_1^0} = 223 \text{ GeV} \quad (62)$$

$$m_{H_2^\pm} = m_{A_2^0} = 305 \text{ GeV} \quad (63)$$

$$m_{H^{++}} = m_{A_3^0} = m_{H_3^\pm} = 195 \text{ GeV} \quad (64)$$

$$m_{H_1^0} = 139 \text{ GeV} \quad m_{H_2^0} = 275 \text{ GeV} \quad (65)$$

as shown in Fig. 10. This model satisfies the perturbativity and vacuum stability constraints

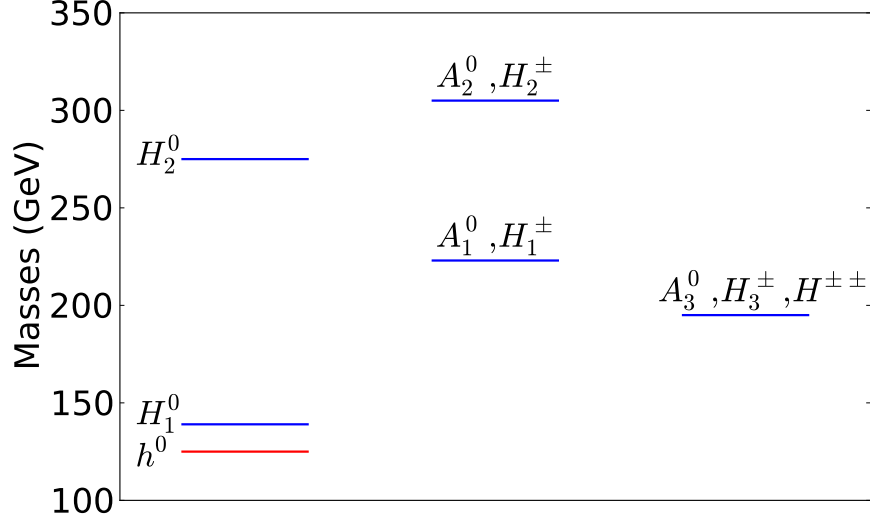


FIG. 10: Higgs masses for the benchmark model described in Sec. 3.4.2. The observed 125 GeV Higgs is shown in red.

up to $\Lambda \sim 7$ TeV. Details about the corresponding quartic couplings can be found in Appendix B.

The branching ratios for the 125 GeV Higgs become:

$$\text{Br}(h \rightarrow bb) = 0.34 \quad \text{Br}(h \rightarrow WW) = 0.46 \quad (66)$$

$$\text{Br}(h \rightarrow ZZ) = 0.056 \quad \text{Br}(h \rightarrow \gamma\gamma) = 0.012 \quad (67)$$

The production cross sections in the gluon and vector boson fusion channels are

$$\sigma(gg \rightarrow h) = 5.9 \text{ pb} \quad \sigma(VV \rightarrow h) = 1.0 \text{ pb} \quad (68)$$

and the signal strength in the $h \rightarrow ZZ \rightarrow 4l$ and the $h \rightarrow \gamma\gamma$ channels are

$$\mu(h \rightarrow ZZ \rightarrow 4l) = 0.70 \quad \mu(h \rightarrow \gamma\gamma) = 1.67 \quad (69)$$

The corresponding signal strengths for H_1^0 and H_2^0 when no alternate decay modes are introduced are

$$\mu(H_1 \rightarrow ZZ \rightarrow 4l) = 2.1 \quad \mu(H_1 \rightarrow \gamma\gamma) = 1.46 \quad (70)$$

$$\mu(H_2 \rightarrow ZZ \rightarrow 4l) = 0.47 \quad (71)$$

while the corresponding ATLAS [25] and CMS [56] upper bounds are

$$\mu_{ZZ}^{\text{CMS}}(m_{H_1^0}) < 0.13 \quad \mu_{\gamma\gamma}^{\text{ATLAS}}(m_{H_1^0}) < 0.74 \quad (72)$$

$$\mu_{ZZ}^{\text{CMS}}(m_{H_2^0}) < 0.30 \quad (73)$$

Introducing a SM scalar singlet S , which couples to the h_1 interaction eigenstate via the operator

$$\mathcal{L} = \lambda_1 h_1^\dagger h_1 S^\dagger S \quad (74)$$

allows to reduce the different signal strength down to below the ATLAS and CMS bounds. For

$$\lambda_1 = 0.2 \quad m_S = 66 \text{ GeV}, \quad (75)$$

the signal strengths for H_1^0 and H_2^0 become

$$\mu(H_1 \rightarrow ZZ \rightarrow 4l) = 0.024 \quad \mu(H_1 \rightarrow \gamma\gamma) = 0.017 \quad (76)$$

$$\mu(H_2 \rightarrow ZZ \rightarrow 4l) = 0.25 \quad (77)$$

The charged Higgs are dominantly produced in association with a top quark through $gb \rightarrow tH^-$, with cross sections of the order of the picobarn, and dominantly decay to tb and Wh [67, 68]. Since the decay to tb suffers from high background rates, current searches focus on rare decays to $\tau\nu$ [69] and cs [70], giving weak exclusion bounds. Since these rare decays are further suppressed in our model by the fact that only one Higgs interaction eigenstate couples to leptons and light quarks, current charged Higgs searches are far from excluding our benchmark model. Associated production of a charged Higgs with a top quark can lead to final states of the form $t\bar{t}b$ and could therefore be probed using $t\bar{t}$ cross section measurements. However, the current uncertainties set by ATLAS and CMS on the top pair production cross section at 8 TeV are of the order of 10 pb and deviations due to the associated production of charged Higgses would not be visible [71, 72]. Pair production of charged Higgses occurs only through electroweak processes, with cross sections of the order of 10 fb. Although these processes lead to more characteristic final states, SM backgrounds involving top quarks and gauge bosons would be largely dominating.

The doubly-charged Higgs can decay only to a pair of same-sign W bosons, which can produce signals with same-sign lepton pairs. Searches for such signatures would have particularly low background rates, and could lead to strong constraints on the doubly-charged Higgs mass, in spite of its low production rate. Existing LHC [73, 74] and Tevatron [75, 76] searches for these particles, however, consider only direct decays to same-sign lepton pairs. Recasting these searches to look for doubly-charged Higgses decaying to vector bosons has been done in [77] and gives only weak bounds. Since the doubly-charged Higgs does not couple to leptons, it would be dominantly produced electroweakly, in association with a charged Higgs, with a cross section of the order of 10 pb. The corresponding final states are similar to the ones probed by the CMS and ATLAS SUSY searches for a same-sign lepton pair produced with jets [72, 78]. The number of observed events, however, would be too small to lead to significant excesses in the signal regions of interest. Dedicated searches for doubly-charged Higgses decaying to W pairs have been designed in [53, 79, 80] and seem to indicate that, for masses comparable to ours, a discovery could be made with the current 8 TeV dataset.

4. DISCUSSION

This article investigates the different low energy scenarios that could lead to the negative values of the top Yukawa coupling still allowed by the ATLAS Higgs searches. We focus on three possible scenarios involving either new vector-like top partners or new Higgs-like scalars. In order for the new physics contribution to the top Yukawa to be large enough, the new particles have to be light and have large couplings to the top quark. Scenarios with new vector-like top partners and a negative top Yukawa are therefore either excluded by the current LHC searches or leading to low scale Landau poles. Viable models with additional Higgs-like scalars have to include additional scalar doublets and triplets which heavily mix with each other. One possible scenario which is still allowed by the current ATLAS and Tevatron Higgs searches is a Georgi-Machacek model with one additional Higgs doublet. This model would predict a large number of new charged and neutral Higgses with sizable couplings to the top quark. Designing new LHC searches or recasting existing ones would

allow to strongly constrain the corresponding parameter space, even with the current 8 TeV dataset.

Acknowledgements

SE and JW are supported by the US DOE under contract number DE-AC02-76-SF00515. SE is supported by a Stanford Graduate Fellowship. Fermilab is operated by Fermi Research Alliance, LLC under Contract No. DE-AC02-07CH11359 with the United States Department of Energy.

Appendix A: RGEs for the 2HDM

The Higgs potential for a general two Higgs doublet model (2HDM) is where

$$h_1 = \left(\frac{G^\pm \cos \beta + H^\pm \sin \beta}{v \cos \beta + h_1^0 + i(G^0 \cos \beta + A^0 \sin \beta)} \right) \quad h_2 = \left(\frac{-G^\pm \sin \beta + H^\pm \cos \beta}{v \sin \beta + h_2^0 + i(-G^0 \sin \beta + A^0 \cos \beta)} \right) \quad (\text{A1})$$

Both Higgs doublets couple to the top quark

$$\mathcal{L}_{\text{Yukawa}} = y_t h Q u^c + y'_t H Q u^c \quad (\text{A2})$$

The most general Higgs potential in the 2HDM can be expressed as

$$\begin{aligned} V = & m_1^2 h_1^\dagger h_1 + m_2^2 h_2^\dagger h_2 + m_{12}^2 (h_1^\dagger h_2 + \text{c.c.}) \\ & + \frac{\lambda_1}{2} (h_1^\dagger h_1)^2 + \frac{\lambda_2}{2} (h_2^\dagger h_2)^2 + \lambda_3 (h_1^\dagger h_1)(h_2^\dagger h_2) + \lambda_4 (h_1^\dagger h_2)(h_2^\dagger h_1) \\ & + \frac{\lambda_5}{2} \left[(h_1^\dagger h_2)^2 + \text{c.c.} \right] + \lambda_6 \left[(h_1^\dagger h_1)(h_1^\dagger h_2) + \text{c.c.} \right] + \lambda_7 \left[(h_2^\dagger h_2)(h_2^\dagger h_1) + \text{c.c.} \right] \end{aligned} \quad (\text{A3})$$

The beta functions for the Yukawa and quartic couplings are then (neglecting the $SU(2) \times U(1)$ couplings)

$$\begin{aligned}
16\pi^2\beta_{\lambda_1} &= 12\lambda_1^2 + 4\lambda_3^2 + 4\lambda_3\lambda_4 + 2\lambda_4^2 + 2\lambda_5^2 + 24\lambda_6^2 + 12\lambda_1y_t^2 + 12\lambda_6y_ty_t' - 12y_t^4 \\
16\pi^2\beta_{\lambda_2} &= 12\lambda_2^2 + 4\lambda_3^2 + 4\lambda_3\lambda_4 + 2\lambda_4^2 + 2\lambda_5^2 + 24\lambda_7^2 + 12\lambda_2y_t'^2 + 12\lambda_7y_ty_t' - 12y_t'^4 \\
16\pi^2\beta_{\lambda_3} &= (\lambda_1 + \lambda_2)(6\lambda_3 + 2\lambda_4) + 4\lambda_3^2 + 2\lambda_4^2 + 2\lambda_5^2 + 4\lambda_6^2 + 16\lambda_6\lambda_7 + 4\lambda_7^2 \\
&\quad + 6\lambda_3(y_t^2 + y_t'^2) + 6(\lambda_6 + \lambda_7)y_ty_t' - 12y_t^2y_t'^2 \\
16\pi^2\beta_{\lambda_4} &= 2(\lambda_1 + \lambda_2)\lambda_4 + 8\lambda_3\lambda_4 + 4\lambda_4^2 + 8\lambda_5^2 + 10\lambda_6^2 + 4\lambda_6\lambda_7 + 10\lambda_7^2 \\
&\quad + 6\lambda_4(y_t^2 + y_t'^2) + 6(\lambda_6 + \lambda_7)y_ty_t' - 12y_t^2y_t'^2 \\
16\pi^2\beta_{\lambda_5} &= 2(\lambda_1 + \lambda_2)\lambda_5 + 8\lambda_3\lambda_5 + 12\lambda_4\lambda_5 + 10\lambda_6^2 + 4\lambda_6\lambda_7 + 10\lambda_7^2 \\
&\quad + 6\lambda_5(y_t^2 + y_t'^2) + 6(\lambda_6 + \lambda_7)y_ty_t' - 12y_t^2y_t'^2 \\
16\pi^2\beta_{\lambda_6} &= 12\lambda_1\lambda_6 + 6\lambda_3(\lambda_6 + \lambda_7) + 8\lambda_4\lambda_6 + 4\lambda_4\lambda_7 + 10\lambda_5\lambda_6 + 2\lambda_5\lambda_7 \\
&\quad + 9\lambda_6y_t^2 + 3\lambda_6y_t'^2 + 3(\lambda_1 + \lambda_3 + \lambda_4 + \lambda_5)y_ty_t' - 12y_t^3y_t' \\
16\pi^2\beta_{\lambda_7} &= 12\lambda_2\lambda_7 + 6\lambda_3(\lambda_6 + \lambda_7) + 8\lambda_4\lambda_7 + 4\lambda_4\lambda_6 + 10\lambda_5\lambda_7 + 2\lambda_5\lambda_6 \\
&\quad + 9\lambda_7y_t'^2 + 3\lambda_7y_t^2 + 3(\lambda_2 + \lambda_3 + \lambda_4 + \lambda_5)y_ty_t' - 12y_t^3y_t' \\
16\pi^2\beta_{y_t} &= y_t \left(\frac{9}{2}y_t^2 + \frac{3}{2}y_t'^2 - 8g_3^2 \right) + 3y_ty_t'^2 \\
16\pi^2\beta_{y_t'} &= y_t' \left(\frac{9}{2}y_t'^2 + \frac{3}{2}y_t^2 - 8g_3^2 \right) + 3y_t^2y_t' \\
16\pi^2\beta_{g_3} &= -7g_3^3
\end{aligned}$$

The stability conditions are given by [81]

$$\lambda_1 > 0, \quad \lambda_2 > 0, \quad \lambda_3 > -2\sqrt{\lambda_1\lambda_2} \quad (\text{A4})$$

$$\lambda_3 + \frac{\lambda_4 + \lambda_5}{2} > -2\sqrt{\lambda_1\lambda_2} \quad (\text{A5})$$

$$\lambda_3 + \frac{\lambda_4 - \lambda_5}{2} > -2\sqrt{\lambda_1\lambda_2} \quad (\text{A6})$$

$$\lambda_1 + \lambda_2 + \lambda_3 + \frac{\lambda_4 + \lambda_5}{2} - 2|\lambda_6 + \lambda_7| > 0 \quad (\text{A7})$$

Appendix B: The Georgi-Machacek model

Let us consider the following Higgs potential

$$\begin{aligned}
V = & \frac{1}{2}m_{11}\mathcal{H}_{11}^\dagger\mathcal{H}_{11} + \frac{1}{2}m_{22}\mathcal{H}_{22}^\dagger\mathcal{H}_{22} + \frac{1}{2}m_{12}\mathcal{H}_{12}^\dagger\mathcal{H}_{12} + \frac{1}{8}\lambda_1\left(\mathcal{H}_{11}^\dagger\mathcal{H}_{11}\right)^2 \\
& + \frac{1}{8}\lambda_2\left(\mathcal{H}_{22}^\dagger\mathcal{H}_{22}\right)^2 + \frac{1}{4}\lambda_3\left(\mathcal{H}_{11}^\dagger\mathcal{H}_{11}\right)\left(\mathcal{H}_{22}^\dagger\mathcal{H}_{22}\right) + \frac{1}{4}\lambda_4\left(\mathcal{H}_{12}^\dagger\mathcal{H}_{12}\right)\left(\mathcal{H}_{21}^\dagger\mathcal{H}_{21}\right) \\
& + \frac{1}{8}\lambda_5\left(\mathcal{H}_{12}^\dagger\mathcal{H}_{12}\right)^2 + \frac{1}{4}\lambda_6\left(\mathcal{H}_{11}^\dagger\mathcal{H}_{11}\right)\left(\mathcal{H}_{12}^\dagger\mathcal{H}_{12}\right) + \frac{1}{4}\lambda_7\left(\mathcal{H}_{22}^\dagger\mathcal{H}_{22}\right)\left(\mathcal{H}_{12}^\dagger\mathcal{H}_{12}\right) \\
& - \mu\text{Tr}\left(\mathcal{H}_{11}^\dagger\frac{\tau_a}{2}\mathcal{H}_{11}\frac{\tau_b}{2}\right)(P^\dagger\Delta P)^{ab} \\
& + \text{c.c.}
\end{aligned} \tag{B1}$$

To make the custodial invariance manifest, the Higgs doublets and triplets are represented using the matrices \mathcal{H}_{ij} and Δ respectively, with

$$\mathcal{H}_{ij} = \begin{pmatrix} h_i^{0*} & h_j^+ \\ -h_i^- & h_j^0 \end{pmatrix} \quad \Delta = \begin{pmatrix} \chi^{0*} & \xi^+ & \chi^{++} \\ \chi^- & \xi^0 & \xi^+ \\ \chi^{--} & \xi^- & \chi^0 \end{pmatrix} \tag{B2}$$

The τ_i are the Pauli matrices and P is given by

$$P = \begin{pmatrix} -\frac{i}{\sqrt{2}} & \frac{i}{\sqrt{2}} & 0 \\ \frac{i}{\sqrt{2}} & -\frac{i}{\sqrt{2}} & 0 \\ 0 & 0 & 1 \end{pmatrix} \tag{B3}$$

The fields h_1^0 , h_2^0 , ξ^0 and χ^0 can take vevs

$$h_1^0 = \frac{v_h \cos \beta + h^0 + i(G^0 \cos \beta + A^0 \sin \beta)}{\sqrt{2}} \tag{B4}$$

$$h_2^0 = \frac{v_h \sin \beta + H^0 + i(-G^0 \sin \beta + A^0 \cos \beta)}{\sqrt{2}} \tag{B5}$$

$$\chi_0 = v_\chi + \frac{\chi_r + i\chi_i}{\sqrt{2}}, \quad \xi_0 = v_\xi + \xi_r \tag{B6}$$

We also define

$$h_1^\pm = G^\pm \cos \beta + H_0^\pm \sin \beta \tag{B7}$$

$$h_2^\pm = H_0^\pm \cos \beta - G^\pm \sin \beta \tag{B8}$$

For our model to remain invariant under custodial symmetry $SU(2)_C$, we need

$$v_\xi = v_\chi = v_\Delta \quad (\text{B9})$$

and therefore, we define

$$v_\Delta = v \sin \alpha \quad v_h = v \cos \alpha \quad (\text{B10})$$

The nine fields contained in Δ can be decomposed in one $SU(2)_C$ singlet H_1 , one triplet H_3 and one five-plet H_5 defined by

$$H_5^{\pm\pm} = \chi^{\pm\pm} \quad H_5^\pm = \frac{1}{\sqrt{2}}(\chi^\pm - \xi^\pm) \quad H_5^0 = \frac{1}{\sqrt{3}}(\chi_r - \sqrt{2}\xi_r) \quad (\text{B11})$$

$$H_3^\pm = \frac{1}{\sqrt{2}}(\chi^\pm + \xi^\pm) \quad H_3^0 = \chi_i \quad H_1^0 = \frac{1}{\sqrt{3}}(\xi_r + \sqrt{2}\chi_r) \quad (\text{B12})$$

The members of the $SU(2)_C$ five-plet H_5 do not mix with any other field and their mass is

$$m_5 = \frac{\mu v_h^2 \cos^2 \beta}{4v_\Delta} \quad (\text{B13})$$

The mass matrices for the other fields are given in the (H_1^0, h_1^0, h_2^0) basis for the CP-even scalars, (H_3^0, G^0, A^0) basis for the CP-odd scalars, and $(H_3^\pm, G^\pm, H_0^\pm)$ basis for the charged scalars

$$M_{\text{charged}} = \begin{pmatrix} \frac{\mu v_h^2 \cos^2 \beta}{4v_\Delta} & -\frac{v_h \mu \cos^2 \beta}{\sqrt{2}} & \frac{v_h \mu \cos \beta \sin \beta}{\sqrt{2}} \\ -\frac{v_h \mu \cos^2 \beta}{\sqrt{2}} & 2v_\Delta \mu \cos^2 \beta & -v_\Delta \mu \sin(2\beta) \\ \frac{v_h \mu \cos \beta \sin \beta}{\sqrt{2}} & -v_\Delta \mu \sin(2\beta) & m_{H_0^\pm}^2 \end{pmatrix} \quad (\text{B14})$$

$$M_{\text{CP-odd}} = \begin{pmatrix} \frac{\mu v_h^2 \cos^2 \beta}{4v_\Delta} & -\frac{v_h \mu \cos^2 \beta}{\sqrt{2}} & \frac{v_h \mu \cos \beta \sin \beta}{\sqrt{2}} \\ -\frac{v_h \mu \cos^2 \beta}{\sqrt{2}} & 2v_\Delta \mu \cos^2 \beta & -v_\Delta \mu \sin(2\beta) \\ \frac{v_h \mu \cos \beta \sin \beta}{\sqrt{2}} & -v_\Delta \mu \sin(2\beta) & m_{A^0}^2 \end{pmatrix} \quad (\text{B15})$$

$$M_{\text{CP-even}} = \begin{pmatrix} \frac{\mu v_h^2 \cos^2 \beta}{4v_\Delta} & -\frac{\sqrt{3}}{2} \mu v_h \cos \beta & 0 \\ -\frac{\sqrt{3}}{2} \mu v_h \cos \beta & m_{h^0}^2 & m_{12}^2 \\ 0 & m_{12}^2 & m_{H^0}^2 \end{pmatrix} \quad (\text{B16})$$

where

$$m_{h_0} = \lambda_1 \cos^2 \beta + \lambda_6 \sin 2\beta - \frac{m_{22}}{v^2} \tan^2 \beta \quad (\text{B17})$$

$$+ \sin^2 \beta \left(\frac{\lambda_3 + \lambda_4 + \lambda_5}{2} + \lambda_7 \tan \beta + \frac{\lambda_2}{2} \tan^2 \beta \right) \\ m_{H_0} = -\frac{m_{22}}{v^2} + \frac{\lambda_3 + \lambda_4 + \lambda_5}{2} \cos^2 \beta + \frac{3}{2} \lambda_7 \sin 2\beta + \frac{3}{2} \lambda_2 \sin^2 \beta \quad (\text{B18})$$

$$m_{12} = \lambda_6 \cos^2 \beta + \frac{\lambda_3 + \lambda_4 + \lambda_5}{4} \sin 2\beta + \left(\frac{m_{22}}{v^2} - \frac{\lambda_2}{2} \sin^2 \beta \right) \tan \beta \quad (\text{B19})$$

Both Higgs doublets couple to the top quark similarly as in the 2HDM shown in App. A. The RGEs for the quartic and Yukawa couplings are also the same as in this model.

Defining the mixing angles θ and γ such as the 125 GeV Higgs mass eigenstate is defined by

$$h^0 = h_1^0 \sin \gamma \cos \theta + h_2^0 \sin \gamma \sin \theta + H_1^0 \cos \gamma, \quad (\text{B20})$$

the values of the top Yukawa couplings y and y' at the top quark scale are

$$y = -\frac{y_{SM}}{\sin \theta} \left(\kappa_t \frac{\sin \beta}{\sin \gamma} - \frac{\sin \theta}{\cos \alpha} \right) \quad (\text{B21})$$

$$y' = \frac{y_{SM}}{\sin \theta} \left(\kappa_t \frac{\cos \beta}{\sin \gamma} - \frac{\cos \theta}{\cos \alpha} \right) \quad (\text{B22})$$

We can also express μ in function of the mixing angles α , β , γ and θ

$$\mu = \frac{m_h^2}{v \cos \alpha \cos \beta} \frac{2}{\sqrt{2} \cot \alpha \cos \beta - \sqrt{3} \tan \gamma \cos \theta} \quad (\text{B23})$$

The parameters for the benchmark model mentioned in Sec. 3.4 are

$$\beta = 0.20 \quad \theta = 1.16 \quad \gamma = 1.12 \quad \alpha = 0.52 \quad (\text{B24})$$

$$\lambda_1 = 1.12 \quad \lambda_2 = 0.27 \quad \lambda_3 = 2.33 \quad \lambda_4 = -1.01 \quad \lambda_5 = -1.01 \quad \lambda_6 = 0 \quad \lambda_7 = -1.60$$

Appendix C: RGEs for yukawa couplings with one top partner and one scalar singlet

The RGEs for a Lagrangian of the type

$$\mathcal{L}_{\text{int}} = y_0 H q_3 u^c + y_2 H q_3 U^c + y_1 S U u^c + M_1 U U^c \quad (\text{C1})$$

where S is taken to be a complex scalar, are

$$16\pi^2 \frac{dy_0}{d\log\mu} = y_0 \left[\frac{9}{2}(y_0^2 + y_2^2) + \frac{1}{2}y_1^2 - 8g_3^2 \right] \quad (\text{C2})$$

$$16\pi^2 \frac{dy_2}{d\log\mu} = y_2 \left[\frac{9}{2}(y_0^2 + y_2^2) + \frac{1}{2}y_1^2 - 8g_3^2 \right] \quad (\text{C3})$$

$$16\pi^2 \frac{dy_1}{d\log\mu} = y_1 [4y_1^2 + y_0^2 + y_2^2 - 8g_3^2] \quad (\text{C4})$$

$$16\pi^2 \frac{dg_3}{d\log\mu} = -\frac{19}{3}g_3^3 \quad (\text{C5})$$

therefore

$$y_2(t) = \frac{y_2(0)}{y_0(0)} y_0(t) \quad (\text{C6})$$

$$(\text{C7})$$

The RGEs would then become

$$16\pi^2 \frac{dy_0}{d\log\mu} = y_0 \left[\frac{9}{2}y_0^2(1 + \mathcal{K}^2) + \frac{1}{4}y_1^2 - 8g_3^2 \right] \quad (\text{C8})$$

$$16\pi^2 \frac{dy_1}{d\log\mu} = y_1 [4y_1^2 + (1 + \mathcal{K}^2)y_0^2 - 8g_3^2] \quad (\text{C9})$$

$$16\pi^2 \frac{dg_3}{d\log\mu} = -\frac{19}{3}g_3^3 \quad (\text{C10})$$

where

$$\mathcal{K} = \frac{y_2(0)}{y_0(0)} \quad (\text{C11})$$

which gives

$$16\pi^2 \frac{dy}{d\log\mu} \gtrsim \frac{9}{2}(\mathcal{K}^2 + 1)y_0^3 \quad (\text{C12})$$

$$16\pi^2 \frac{d|y_1|}{d\log\mu} \gtrsim 4|y_1|^3 \quad (\text{C13})$$

so in order to have Landau poles appear only above 10 TeV, we need

$$y_0(0) \lesssim \frac{2.1}{\sqrt{1 + \mathcal{K}^2}} \quad (\text{C14})$$

$$y_1(0) \lesssim 2.2 \quad (\text{C15})$$

Eq. 13 gives

$$\mathcal{K}^2 = \left(1 - \frac{y_{SM}^2}{y_0^2(0)}\right) \left(\frac{m_T^2 y_{SM}^2}{m_t^2 y_0^2(0)} - 1\right) \quad (\text{C16})$$

which leaves us with

$$(y_0^2(0) - y_{SM}^2) \left(\frac{m_T^2 y_{SM}^2}{m_t^2 y_0^2(0)} - 1\right) + y_0^2(0) \lesssim 2.1^2 \quad (\text{C17})$$

Appendix D: RGEs for yukawa couplings with two additional top partners

The RGEs for a Lagrangian of the type

$$\mathcal{L}_{\text{int}} = y_0 H q_3 u^c + y_1 H q_3 U^c + y_2 H Q U^c + y_3 H Q u^c + M_1 U U^c + M_2 Q Q^c \quad (\text{D1})$$

are

$$16\pi^2 \frac{dy_0}{d\log \mu} = y_0 \left[\frac{9}{2}(y_0^2 + y_1^2 + y_3^2) + 3y_2^2 - 8g_3^2 \right] + \frac{3}{2}y_1 y_2 y_3 \quad (\text{D2})$$

$$16\pi^2 \frac{dy_1}{d\log \mu} = y_1 \left[\frac{9}{2}(y_0^2 + y_1^2 + y_2^2) + 3y_3^2 - 8g_3^2 \right] + \frac{3}{2}y_0 y_2 y_3 \quad (\text{D3})$$

$$16\pi^2 \frac{dy_2}{d\log \mu} = y_2 \left[\frac{9}{2}(y_1^2 + y_2^2 + y_3^2) + 3y_0^2 - 8g_3^2 \right] + \frac{3}{2}y_0 y_1 y_3 \quad (\text{D4})$$

$$16\pi^2 \frac{dy_3}{d\log \mu} = y_3 \left[\frac{9}{2}(y_0^2 + y_2^2 + y_3^2) + 3y_1^2 - 8g_3^2 \right] + \frac{3}{2}y_0 y_1 y_2 \quad (\text{D5})$$

$$16\pi^2 \frac{dg_3}{d\log \mu} = -\frac{17}{3}g_3^3 \quad (\text{D6})$$

These RGEs can also be expressed as

$$8\pi^2 \frac{d(y_0^2 - y_2^2)}{d\log \mu} = (y_0^2 - y_2^2) \left[\frac{9}{2}(y_0^2 + y_1^2 + y_2^2 + y_3^2) - 8g_3^2 \right] \quad (\text{D7})$$

$$8\pi^2 \frac{d(y_1^2 - y_3^2)}{d\log \mu} = (y_1^2 - y_3^2) \left[\frac{9}{2}(y_0^2 + y_1^2 + y_2^2 + y_3^2) - 8g_3^2 \right] \quad (\text{D8})$$

which gives

$$y_0^2(t) - y_2^2(t) = \mathcal{K}^2 (y_1^2(t) - y_3^2(t)) \quad (\text{D9})$$

where

$$\mathcal{K}^2 = \frac{y_0^2(0) - y_2^2(0)}{y_1^2(0) - y_3^2(0)} \quad t = \log \mu \quad (\text{D10})$$

Therefore, for a given set of initial conditions $\{y_{00}, y_{10}, y_{20}, y_{30}\}$, the configuration for which Landau poles will appear the latest is always

$$|y_{00}| = |y_{01}| = |y_{02}| = |y_{03}| \quad (\text{D11})$$

In this last case, the couplings remain equal at all scales and are therefore described by only one RGE

$$16\pi^2 \frac{dy}{d\log \mu} = 15y^3 - 8yg_3^2 \quad (\text{D12})$$

so Landau poles appear later than 10 TeV if and only if

$$y \lesssim 1.06 \quad (\text{D13})$$

-
- [1] S. Chatrchyan et al. (CMS Collaboration), Phys.Lett. **B716**, 30 (2012), 1207.7235.
 - [2] G. Aad et al. (ATLAS Collaboration), Phys.Lett. **B716**, 1 (2012), 1207.7214.
 - [3] D. Carmi, A. Falkowski, E. Kuflik, and T. Volansky, JHEP **1207**, 136 (2012), 1202.3144.
 - [4] C. Englert, T. Plehn, M. Rauch, D. Zerwas, and P. M. Zerwas, Phys.Lett. **B707**, 512 (2012), 1112.3007.
 - [5] A. Azatov, R. Contino, and J. Galloway, JHEP **1204**, 127 (2012), 1202.3415.
 - [6] J. Espinosa, C. Grojean, M. Muhlleitner, and M. Trott, JHEP **1205**, 097 (2012), 1202.3697.
 - [7] P. P. Giardino, K. Kannike, M. Raidal, and A. Strumia, JHEP **1206**, 117 (2012), 1203.4254.
 - [8] T. Li, X. Wan, Y.-k. Wang, and S.-h. Zhu, JHEP **1209**, 086 (2012), 1203.5083.
 - [9] M. Rauch (2012), 1203.6826.
 - [10] J. Ellis and T. You, JHEP **1206**, 140 (2012), 1204.0464.
 - [11] M. Klute, R. Lafaye, T. Plehn, M. Rauch, and D. Zerwas, Phys.Rev.Lett. **109**, 101801 (2012), 1205.2699.
 - [12] A. Azatov, S. Chang, N. Craig, and J. Galloway, Phys.Rev. **D86**, 075033 (2012), 1206.1058.
 - [13] D. Carmi, A. Falkowski, E. Kuflik, and T. Volansky, Frascati Phys.Ser. **57**, 315 (2013), 1206.4201.

- [14] T. Corbett, O. Eboli, J. Gonzalez-Fraile, and M. Gonzalez-Garcia, Phys.Rev. **D86**, 075013 (2012), 1207.1344.
- [15] P. P. Giardino, K. Kannike, M. Raidal, and A. Strumia, Phys.Lett. **B718**, 469 (2012), 1207.1347.
- [16] M. R. Buckley and D. Hooper, Phys.Rev. **D86**, 075008 (2012), 1207.1445.
- [17] J. Ellis and T. You, JHEP **1209**, 123 (2012), 1207.1693.
- [18] M. Montull and F. Riva, JHEP **1211**, 018 (2012), 1207.1716.
- [19] J. Espinosa, C. Grojean, M. Muhlleitner, and M. Trott, JHEP **1212**, 045 (2012), 1207.1717.
- [20] D. Carmi, A. Falkowski, E. Kuflik, T. Volansky, and J. Zupan, JHEP **1210**, 196 (2012), 1207.1718.
- [21] T. Plehn and M. Rauch, Europhys.Lett. **100**, 11002 (2012), 1207.6108.
- [22] J. R. Espinosa, C. Grojean, V. Sanz, and M. Trott, JHEP **1212**, 077 (2012), 1207.7355.
- [23] Tech. Rep. ATLAS-CONF-2013-034, ATLAS-COM-CONF-2013-035 (2013).
- [24] Tech. Rep. CMS-PAS-HIG-13-005, CERN, Geneva (2013).
- [25] Tech. Rep. ATLAS-CONF-2013-012, ATLAS-COM-CONF-2013-015 (2013).
- [26] T. Aaltonen et al. (CDF Collaboration), Phys.Rev. **D88**, 052013 (2013), 1301.6668.
- [27] A. G. Cohen and M. Schmaltz (2012), 1207.3495.
- [28] I. Dorsner, S. Fajfer, A. Greljo, and J. F. Kamenik, JHEP **1211**, 130 (2012), 1208.1266.
- [29] M. Reece, New J.Phys. **15**, 043003 (2013), 1208.1765.
- [30] T. Lee, Phys.Rev. **D8**, 1226 (1973).
- [31] G. Branco, P. Ferreira, L. Lavoura, M. Rebelo, M. Sher, et al., Phys.Rept. **516**, 1 (2012), 1106.0034.
- [32] J. F. Gunion and H. E. Haber, Phys.Rev. **D67**, 075019 (2003), hep-ph/0207010.
- [33] Tech. Rep. ATLAS-CONF-2013-030, ATLAS-COM-CONF-2013-028 (2013).
- [34] Tech. Rep. ATLAS-CONF-2013-013, ATLAS-COM-CONF-2013-018 (2013).
- [35] Tech. Rep. ATLAS-CONF-2013-010, CERN, Geneva (2013).
- [36] Tech. Rep. CMS-PAS-B2G-12-015, CERN, Geneva (2013).
- [37] N. Arkani-Hamed, A. Cohen, E. Katz, and A. Nelson, JHEP **0207**, 034 (2002), hep-

- ph/0206021.
- [38] T. Han, H. E. Logan, B. McElrath, and L.-T. Wang, Phys.Rev. **D67**, 095004 (2003), hep-ph/0301040.
 - [39] M. Schmaltz and D. Tucker-Smith, Ann.Rev.Nucl.Part.Sci. **55**, 229 (2005), hep-ph/0502182.
 - [40] L. Randall and R. Sundrum, Phys.Rev.Lett. **83**, 3370 (1999), hep-ph/9905221.
 - [41] M. E. Machacek and M. T. Vaughn, Nucl.Phys. **B236**, 221 (1984).
 - [42] Tech. Rep. ATLAS-CONF-2013-018, ATLAS-COM-CONF-2013-024 (2013).
 - [43] Tech. Rep. ATLAS-CONF-2013-079, CERN, Geneva (2013).
 - [44] S. Chatrchyan et al. (CMS Collaboration) (2013), 1310.3687.
 - [45] Tech. Rep. ATLAS-CONF-2012-160, CERN, Geneva (2012).
 - [46] Tech. Rep. CMS-PAS-HIG-13-007, CERN, Geneva (2013).
 - [47] S. Chatrchyan et al. (CMS Collaboration), Phys.Lett. **B713**, 68 (2012), 1202.4083.
 - [48] A. Akeroyd, M. Aoki, and H. Sugiyama (2011).
 - [49] K. Yagyu (2012), 1204.0424.
 - [50] K. Yagyu (2013), 1304.6338.
 - [51] J. Hisano and K. Tsumura, Phys.Rev. **D87**, 053004 (2013), 1301.6455.
 - [52] H. Georgi and M. Machacek, Nucl.Phys. **B262**, 463 (1985).
 - [53] S. Godfrey and K. Moats, Phys.Rev. **D81**, 075026 (2010), 1003.3033.
 - [54] J. Beringer et al. (Particle Data Group), Phys.Rev. **D86**, 010001 (2012).
 - [55] C.-W. Chiang and K. Yagyu, JHEP **1301**, 026 (2013), 1211.2658.
 - [56] (2012).
 - [57] V. Silveira and A. Zee, Phys.Lett. **B161**, 136 (1985).
 - [58] J. McDonald, Phys.Rev. **D50**, 3637 (1994), hep-ph/0702143.
 - [59] C. Burgess, M. Pospelov, and T. ter Veldhuis, Nucl.Phys. **B619**, 709 (2001), hep-ph/0011335.
 - [60] H. Davoudiasl, R. Kitano, T. Li, and H. Murayama, Phys.Lett. **B609**, 117 (2005), hep-ph/0405097.
 - [61] B. Patt and F. Wilczek (2006), hep-ph/0605188.
 - [62] S. Andreas, C. Arina, T. Hambye, F.-S. Ling, and M. H. Tytgat, Phys.Rev. **D82**, 043522

- (2010), 1003.2595.
- [63] M. Raidal and A. Strumia, Phys.Rev. **D84**, 077701 (2011), 1108.4903.
 - [64] X.-G. He and J. Tandean, Phys.Rev. **D84**, 075018 (2011), 1109.1277.
 - [65] A. Drozd, B. Grzadkowski, and J. Wudka, JHEP **1204**, 006 (2012), 1112.2582.
 - [66] Y. Mambrini, Phys.Rev. **D84**, 115017 (2011), 1108.0671.
 - [67] A. Ferrari (ATLAS collaboration), J.Phys.Conf.Ser. **455**, 012016 (2013).
 - [68] M. Flechl (on behalf of the ATLAS Collaboration), PoS **EPS-HEP2011**, 243 (2011), 1307.2045.
 - [69] A. F. Saavedra (ATLAS), PoS **ICHEP2012**, 064 (2013).
 - [70] G. Aad et al. (ATLAS Collaboration), Eur.Phys.J. **C73**, 2465 (2013), 1302.3694.
 - [71] Tech. Rep. ATLAS-CONF-2013-097, ATLAS-COM-CONF-2013-112, CERN, Geneva (2013).
 - [72] Tech. Rep. CMS-PAS-SUS-13-013 (2013).
 - [73] G. Aad et al. (ATLAS Collaboration), Eur.Phys.J. **C72**, 2244 (2012), 1210.5070.
 - [74] Tech. Rep. CMS-PAS-HIG-12-005 (2012).
 - [75] D. Acosta et al. (CDF Collaboration), Phys.Rev.Lett. **93**, 221802 (2004), hep-ex/0406073.
 - [76] V. M. Abazov et al. (D0 Collaboration), Phys.Rev.Lett. **108**, 021801 (2012), 1106.4250.
 - [77] S. Kanemura, K. Yagyu, and H. Yokoya, Phys.Lett. **B726**, 316 (2013), 1305.2383.
 - [78] Tech. Rep. ATLAS-CONF-2013-007, ATLAS-COM-CONF-2013-006 (2013).
 - [79] G. Azuelos, K. Benslama, D. Costanzo, G. Couture, J. Garcia, et al., Eur.Phys.J. **C39S2**, 13 (2005), hep-ph/0402037.
 - [80] C.-W. Chiang, T. Nomura, and K. Tsumura, Phys.Rev. **D85**, 095023 (2012), 1202.2014.
 - [81] P. Ferreira, R. Santos, and A. Barroso, Phys.Lett. **B603**, 219 (2004), hep-ph/0406231.